Biophysical Chemistry 23 (1986) 155–171
Elsevier

BPC 01035

SIMULTANEOUS ANALYSIS OF MULTIPLE FLUORESCENCE DECAY CURVES BY LAPLACE TRANSFORMS

DECONVOLUTION WITH REFERENCE OR EXCITATION PROFILES

M. AMELOOT *, J.M. BEECHEM and L. BRAND

Dept. of Biology, The Johns Hopkins University, Baltimore, MD 21218, U.S.A.

Received 28th July 1985
Accepted 1st October 1985

Key words: Fluorescence decay; Data analysis; Laplace deconvolution; Reference deconvolution

The properties and potentials of the noniterative Laplace deconvolution (LAP2) (M. Ameloot and H. Hendrickx, Biophys. J. 44 (1983) 27) are further investigated. It is shown that LAP2 is exact and that no extrapolations have to be calculated or assumed for the data measured in the actual time window if the impulse response function of the investigated system can be described by a sum of exponentials. The formulas for the LAP2 deconvolution against the measured decay of a reference compound instead of the recorded excitation profile are derived. The procedure for the simultaneous analysis of multiple fluorescence decay curves by LAP2 is described in detail. This global analysis allows one to link any decay parameter, is fast and compares favorably with the nonlinear least-squares iterative reconvolution methods. Because of its short computation time the global analysis by LAP2 provides an efficient way to analyze the fluorescence decay surface in terms of decay associated spectra.

1. Introduction

The analysis of fluorescence decay data obtained by pulsed systems has received much interest during the last decade. Because of the finite width of the excitation pulse, a deconvolution has to be performed to extract the parameters of the fluorescent system from the measured data. Various appropriate methods have been suggested which have been extensively reviewed and compared [1–6]. The various approaches can be divided mainly in two groups. Data analysis can be performed either in real time, using least-squares methods [7,8], or in transform domains, using the method of moments [9], Fourier transforms [10–12], Laplace transforms [10,13,14], modulating functions [15] or the phase plane method [16].

Simultaneous analysis of related fluorescence decay experiments has been suggested for the resolution of fluorescence spectra [17,18] and to improve the accuracy of the recovered parameters [19,20a]. The underlying principle of this methodology is to utilize the relationships between decay curves by linking the common model parameters in the analysis [20a,20b]. It has been shown that this global approach helps both in discerning competing models and in the recovery of model parameters. This principle has been applied to the analysis of total luminescence decay curves in both real time [20a] and transform domains [14,17,19], or features from both domains may be used [21]. In a similar way, the two decay curves corresponding to the parallel and perpendicular intensity components in a fluorescence polarization experiment can be analyzed simultaneously by nonlinear least squares (NLLS) [22,23] or by Laplace transforms [14]. The NLLS implementation, which al-

* Present address: Limburgs Universitair Centrum, Universitaire Campus, B-3610 Diepenbeek, Belgium.

lows for the analysis of complicated anisotropy decay laws [24,25], has been extended further [26].

Global analysis of multiple fluorescence decay curves may lead to situations involving several hundred independent parameters. Because of the iterative character of NLLS and because each fluorescence decay curve contains many data points, this method may require extensive computer time and memory. The recently described noniterative Laplace method (LAP2) [14] is well suited for global analysis. LAP2 has a high-speed performance and requires no initial guesses for the parameter values. It has previously been demonstrated that LAP2 performs well on single-curve analysis and with a combination of a small number of experiments [14].

The aim of this paper is to generalize the theory of LAP2 and to show how it can be used in a global analysis of any number of experiments. The performance of the global analysis by LAP2 will be demonstrated on real and simulated data sets. As a typical application of global analysis, an alternative implementation for decay associated spectra (DAS) [17,27] will be discussed. It will also be shown that the convenience of the LAP2 method can be enhanced by deconvolution against the decay of a reference compound instead of the recorded instrumental response function. This approach, which circumvents the wavelength dependence of the apparatus, has been described for other methods of analysis [28–31].

2. Theory

2.1. Principles of the Laplace deconvolution (single-curve analysis)

In the following it will be assumed that the fluorescent sample under study behaves as a linear system. In an ideal experimental environment the time dependence of the fluorescence $g(t)$ resulting from an excitation pulse $l(t)$ can then be written as a convolution product of $l(t)$ and the impulse response function $f(t)$ of the fluorescent system,

$$g(t) = \int_0^t l(u) f(t-u)\, \mathrm{d}u = l(t) f(t) \tag{1}$$

The function $f(t)$ has to be determined from the measurement of $g(t)$ and $l(t)$. In many cases $f(t)$ can be described adequately by a sum of exponential decaying functions,

$$f(t) = \sum_{i=1}^{n} a_i e^{-t/\tau_i} \tag{2}$$

The problem is then reduced to the estimation of the parameters $\boldsymbol{a} = (a_1, \ldots, a_n)$ and $\boldsymbol{\tau} = (\tau_1, \ldots, \tau_n)$.

Gafni et al. [13] indicated how the Laplace transformation [32] of eq. 1 can be used to recover $\boldsymbol{a}$ and $\boldsymbol{\tau}$. However, an iterative procedure was required because the transformation involves an interpretation beyond the actual time window of the experiment.

Recently, a noniterative Laplace deconvolution (LAP2) was introduced [14]. This implementation is based on restricted transformations of $g(t)$ and $l(t)$. For a function $p(t)$ on the interval $[0, T]$, this transformation $\boldsymbol{L}^T$ is defined by

$$\boldsymbol{L}^T(p) \equiv P^T(s) = \int_0^T p(t) e^{-st}\, \mathrm{d}t \tag{3}$$

In the noniterative method LAP2, the parameters $\boldsymbol{a}$ and $\boldsymbol{\tau}$ are determined from systems of equations of the following form:

$$\frac{G^T(s_j)}{L^T(s_j)} = \sum_{i=1}^{n} \frac{a_i}{s + (1/\tau_i)} \left[1 - \frac{e^{-s_j T} c_i}{L^T(s_j)} \right] \tag{4}$$

where

$$c_i = \int_0^T l(u) e^{-(t-u)/\tau_i}\, \mathrm{d}u \tag{5}$$

Although in the initial development of LAP2, $l(t)$ was assumed to take zero value for $t > T$, eq. 4 is completely general. It is shown in appendix A that eq. 4 is exact without any approximation or extrapolation. In the first presentation of LAP2, the explicit expressions for obtaining a and τ were only given for $n = 1, 2, 3$. The equations for general n are derived in appendix B. For equidistant values of the transform parameters s_j, i.e., $s_{j+k} = s_j + k\Delta$, $\Delta > 0$, the system of eqs. 4 can be rewrit-

ten as

$$\sum_{i=1}^{n} M_{i,n}\left[G^T(s_j)\right] D_i(\tau) = \sum_{i=1}^{n} M_{i-1,n}\left[L^T(s_j)\right] E_i(\boldsymbol{a}, \tau), \quad (6)$$

$$j = 1, \ldots, 2n,$$

where for $1 \leqslant i \leqslant n$

$$E_i(\boldsymbol{a}, \tau) = \sum_{1 \leqslant k_1 < k_2 < \ldots < k_i \leqslant n} \tau_{k_1}\tau_{k_2}\ldots\tau_{k_1} \times (a_{k_1} + a_{k_2} + \ldots + a_{k_i}), \quad (7)$$

$$D_i(\tau) = \sum_{1 \leqslant k_1 < k_2 < \ldots < k_i \leqslant n} \tau_{k_1}\tau_{k_2}\ldots\tau_{k_i}, \quad (8)$$

and

$$D_0(\tau) \equiv 1 \quad (9)$$

The operation $M_{i,n}$ on a transform $P^T(s)$ is defined by

$$M_{i,n}\left[P^T(s_j)\right] \equiv \sum_{k=0}^{n} (-1)^k \frac{n!}{j!(n-j)!} P^T(s_{j+k}) \times s_{j+k}^{i} e^{k\Delta T} \quad (10)$$

The system defined by eq. 6 is linear in the variables $E_i(\boldsymbol{a}, \tau)$ and $D_i(\tau)$. Once their values are obtained, the decay parameters are recovered as follows. The relaxation times τ_i are the roots of the polynomial of degree n,

$$\sum_{i=0}^{n} (-1)^i D_i(\tau)\tau^{n-i} \quad (11)$$

Once τ is determined, $\boldsymbol{a}$ is readily obtained from $E_i(\boldsymbol{a}, \tau)$ by solving a linear system.

The Laplace deconvolution method allows correction for several instrumental artifacts. The scatter contribution S_c can be estimated from

$$\sum_{i=0}^{n} M_{i,n}\left[G^T(s_j)\right] D_i(\tau) = M_{n,n}\left[L^T(s_j)\right] S_c D_n(\tau) + \sum_{i=1}^{n} M_{i-1,n}\left[L^T(s_j)\right] K_i(\boldsymbol{a}, \tau, S_c),$$

$$j = 1, \ldots, 2n+1, \quad (12)$$

with

$$K_i(\boldsymbol{a}, \tau, S_c) = E_i(\boldsymbol{a}, \tau) + S_c D_{i-1}(\tau) \quad (13)$$

An approximate correction for the wavelength dependence of the detection photomultiplier can be obtained by shifting the experimental decay curve with respect to the recorded excitation [13]. The time-shift error Q can be taken into account by replacing $G^T(s_j)$ by $G_Q^T(s_j)$,

$$G_Q^T(s_j) = G^T(s_j) e^{Qs_j} \quad (14)$$

2.2. Simultaneous analysis of multiple decay curves

We now describe the procedure for the simultaneous analysis by LAP2 of multiple decay curves which have some parameters in common. Consider a set of q experiments. For each experiment k consisting of the instrumental response function $l_k(t)$ and the recorded fluorescence $g_k(t)$ one has

$$\sum_{i=1}^{n_k} \boldsymbol{D}_{k,i}(s_j) D_{k,i} - \sum_{i=1}^{n_k} \boldsymbol{E}_{k,i}(s_j) E_{k,i} = -\boldsymbol{D}_{k,0}(s_j) \quad (15)$$

with

$$\boldsymbol{E}_{k,i}(s_j) = M_{i-1,n}\left[L_k^T(s_j)\right] \quad (16)$$

$$\boldsymbol{D}_{k,i}(s_j) = M_{i,n}\left[G_k^T(s_j)\right] \quad (17)$$

and where $D_{k,i}$ and $E_{k,i}$ are the equivalents of the definitions in eqs. 7 and 8; n_k denotes the number of exponentially decaying functions required in the considered experiment.

For many systems of interest decay curves obtained at several excitation/emission wavelengths will exhibit linked decay times and varying pre-exponential components. This means that each experiment gives rise to different functions $E_{k,i}$ and to equal functions of the lifetimes, i.e., $D_{k,i} = D_i$ for $i = 1, \ldots, n$; $k = 1, \ldots, q$. In this case a system of linear equations has to be solved for $n(q+1)$ unknowns, $\{E_{k,i} \mid k = 1, \ldots, q;\ i = 1, \ldots, n\}$ and $\{D_i \mid i = 1, \ldots, n\}$. The minimum number of equations that has to be constructed from the experimental decay surface depends on the number of experiments and on the number of relaxation times. It is not required that the same number of equa-

tions of the type eq. 6 is generated from each individual experiment. When in total more than $n(q+1)$ equations are calculated the overdetermined system can be solved by applying least squares. Once the values of the functions D_i are obtained, the relaxation times τ_j are determined as indicated in section 2.1. Using the recovered values for τ_j and $E_{k,i}$, the pre-exponentials for experiment k can be found. For the described linkage, each curve is analyzed for the same lifetimes. The pre-exponentials then indicate whether a particular lifetime for the considered experiment contributes to the observed decay.

The global analysis approach in NLLS as described by Knutson et al. [20a] is more general because curves may contain a different number of exponentials and any desired linkage between the parameters is possible. To achieve this with LAP2, one has to solve the system of equations directly for the pre-exponentials and the lifetimes instead of solving for their functions $E_{k,i}$ and $D_{k,i}$. Nonlinear techniques must then be used. This version of the program will be referred to as nonlinear LAP2. Although the nonlinear LAP2 is iterative, it is still a fast method because the numerous data points in the time domain are replaced by a few equations in the transform domain. Furthermore, as will be indicated below, storage of intermediate results in computer memory allows for efficient investigation of alternative linkages. The mapping of the parameters of each experiment into the global parameter vector of the total system becomes more complicated in the general case. A scheme similar to that for NLLS [20a,26] can be used.

2.3. Deconvolution against the decay of a reference solution

The instrumental function $I(t)$ is usually estimated from a measurement at the excitation wavelength of a scatter solution which replaces the sample. However, this procedure ignores the wavelength dependence of the instrument [33]. Several correction schemes have been suggested (for an overview, see, e.g., ref. 6). When the shape of the recorded excitation profile is only weakly wavelength dependent, the described Q-shift correction can be applied [13,34]. The use of a monoexponential decaying reference solution has been suggested to estimate the function $I(t)$ indirectly [33,35]. It has also been shown that the required information about $f(t)$ can be obtained by performing the deconvolution directly against the observed decay of the reference, $g_R(t)$ [28–31,36],

$$g_R(t) = I(t) f_R(t) \tag{18}$$

with

$$f_R(t) = a_R e^{-t/\tau_R} \tag{19}$$

The deconvolution against a reference using LAP2 can be achieved as follows. Combination of the Laplace transforms of eqs. 1 and 18 leads to

$$G(s) = G_R(s) \frac{F(s)}{F_R(s)} \tag{20}$$

When $f(t)$ is given by eq. 2 one obtains

$$G(s) = G_R(s) \frac{s + (1/\tau_R)}{a_R} \sum_{i=1}^{n} \frac{a_i}{s + (1/\tau_i)} \tag{21}$$

or equivalently, by using partial fractions,

$$G(s) = G_R(s) \sum_{i=1}^{n} \frac{b_i}{s + (1/\tau_i)} + G_R(s) b_{n+1} \tag{22}$$

with

$$b_i = \frac{a_i}{a_R} \left(\frac{1}{\tau_R} - \frac{1}{\tau_i} \right) \quad \text{for } i = 1, \ldots, n \tag{23}$$

$$b_{n+1} = \sum_{i=1}^{n} \frac{a_i}{a_R} \tag{24}$$

This means that $g(t)$ can be considered as the sum of a multiexponential decay with the 'excitation' $g_R(t)$ and a 'scatter' contamination expressed by b_{n+1}. The corresponding expression of eq. 22 in the time domain is given by

$$g(t) = \sum_{i=1}^{n} b_i e^{-t/\tau_i} g_R(t) + b_{n+1} g_R(t) \tag{25}$$

This result has been used by several authors [28–31,36]. The reference deconvolution using the restricted Laplace transforms $\boldsymbol{L}^T$ can be realized as follows. As $g_R(t)$ plays the role of $I(t)$, the reference deconvolution can be performed by

straightforward application of eq. 12, yielding

$$\sum_{i=0}^{n} M_{i,n}\left[G^T(s_j)\right] D_i(\tau) = M_{n,n}\left[G_R^T(s_j)\right] b_{n+1} D_n(\tau) + \sum_{i=1}^{n} M_{i-1,n}\left[G_R^T(s_j)\right] K_i(\boldsymbol{b}, \tau, b_{n+1}) \quad (26)$$

As already mentioned for the excitation profile $l(t)$, it is not required that $g_R(t)$ vanishes at the end of the time window so that eq. 26 is generally applicable. This is also indicated in the alternative derivation given in appendix D. It is shown in appendix D that the coefficients $M_{i-1,n}[L^T(s_j)]$ in the various equations can be evaluated in terms of $G_R^T(s_j)$,

$$M_{i-1,n}\left[L^T(s)\right] = \frac{1}{a_R \tau_R}\left\{ M_{i-1,n}\left[G_R^T(s_j)\right] + \tau_R M_{i,n}\left[G_R^T(s_j)\right]\right\} \quad (27)$$

Introducing eq. 27 in eq. 6 gives

$$\sum_{i=0}^{n} M_{i,n}\left[G^T(s_j)\right] D_i(\tau) = \sum_{i=1}^{n}\left\{ M_{i-1,n}\left[G_R^T(s_j)\right] + \tau_R M_{i,n}\left[G_R^T(s_j)\right]\right\} \times E_i(\boldsymbol{a}', \tau), \quad (28)$$

where

$$a_i' = \frac{a_i}{a_R \tau_R} \quad (29)$$

The two approaches expressed by eqs. 26 and 28 are completely equivalent. The resulting equations may be derived from each other. In the actual computer implementation, eq. 28 is used so that the same program can be used for the deconvolution against $l(t)$ by putting τ_R formally equal to zero. Furthermore, this implementation is also convenient in the global analysis of multiple decay curves as has been described above.

In the case that $g(t)$ is contaminated by scattered excitation light, $S_c l(t)$, the deconvolution against $g_R(t)$ can be shown to be

$$g(t) = \sum_{i=1}^{n} b_i e^{-t/\tau_i} g_R(t) + \left(b_{n+1} + \frac{S_c'}{\tau_R}\right) g_R(t) + S_c' \frac{d}{dt} g_R(t) \quad (30)$$

with

$$S_c' = \frac{S_c}{a_R} \quad (31)$$

and where b_i, $i = 1, \ldots, n+1$, are defined by eqs. 23 and 24. The corresponding equation using the transforms $\boldsymbol{L}^T$ can be obtained by combining eqs. 12 and 27.

In principal, it is not strictly required that τ_R is known beforehand as its value can be determined from the system of eqs. 28. However, as has been found by others [29,31], more accurate results are obtained for multiexponential decays when τ_R is known, especially when there is a component with $\tau_i \simeq \tau_R$. This raises the question of the determination of τ_R. Its value may be found from a deconvolution against another monoexponential decay by solving the system formed by eqs. 28 in an iterative way for both lifetimes. Other procedures have been suggested by Zuker et al. [31].

2.4. The resolution of spectra by global analysis

The advantage of using decay information for resolving the fluorescence spectrum of a heterogeneously emitting sample into its components has been utilized in pulse fluorimetry [17,18,27] and phase fluorimetry [37]. Knutson et al. [27] use time windowing to generate time-resolved emission spectra from which the required spectra can be calculated by simple algebraic equations using previously determined fluorescence relaxation times. An alternative method consists of performing a simultaneous analysis of the decay curves collected at the various wavelengths of emission [17,18,26]. This will be the approach we will focus on in this section. The equations for resolving the spectra using a global analysis will be stated explicitly and some specific features will be emphasized.

Assume q species of molecules in the excited state after excitation at wavelength λ_{ex}. The fluo-

rescence relaxation at the emission wavelength λ_{em} due to a delta excitation is given by

$$f(\lambda_{ex}, \lambda_{em}, t) = \sum_{j=1}^{q} \alpha_j(\lambda_{ex}, \lambda_{em}) e^{-t/\tau_j} \qquad (32)$$

The spectral contours $\alpha_j(\lambda_{ex}, \lambda_{em})$ have been called decay associated spectra (DAS) [27]. These spectra reflect the species associated spectra (SAS) only when the species are independent. In the other cases, it is sometimes possible to derive SAS from DAS under specific conditions [27]. For example, the spectrum of the monomer in an excimer reaction can be obtained by adding the pre-exponentials obtained in a DAS analysis. This is particularly useful in intramolecular excimer studies. The DAS global analysis can also be very useful in distinguishing a scatter contribution from a true fluorescence component.

The nature of the problem in the analysis of a DAS experiment is well suited for a global approach: the relaxation times can be linked over the complete decay surface and variations in the pre-exponentials with emission wavelength change the relative contribution of each lifetime component. A specific advantage of the global approach concerns the collection dwell times. It has been shown by Knutson et al. [27] that very short dwell times are sufficient to recover the DAS when the relaxation times are known. In the described global approach for the DAS, the relaxation times will be well determined because they are linked over all decay curves. This means that the simultaneous analysis of decay curves with only a few hundred counts at the peak will reveal the DAS. The curves within the decay surface with a larger total count will have more impact on the final values of the parameters. It is worthwhile mentioning that the recovered pre-exponentials do not require additional normalization to reflect the technical fluorescence spectra. The pre-exponentials at the different wavelengths are properly scaled under the following condition: the ratio of the photons emitted by the excitation source during the collection of the excitation and emission profiles has to be constant at each wavelength. Furthermore, because of the short dwell times the shape of the excitation profile is likely to be the same during the collection of the two histograms in the multichannel analyzer.

3. Materials and methods

3.1. Materials

Anthracene and 2-anilinonaphthalene were purchased from Molecular Probes and 9-cyanoanthracene was delivered by Aldrich. Methanol (ultraviolet spectral grade) was obtained from Burdich & Jackson and cyclohexane (gold label) from Aldrich. All materials were used as supplied. The air-saturated samples were measured at room temperature unless indicated otherwise.

3.2. Instrumentation

The fluorescence decay curves were obtained by the time-correlated single photon counting method using a thyratron gated flashlamp from Photochemical Research Associates. The computerized instrument has been described elsewhere [3,38]. The detection photomultiplier was an Amperex 56 DUVP type.

3.3. Data analysis

3.3.1. Implementation of the LAP2 global analyses

In the LAP2 global analyses, the measured data for all the experiments need not all reside simultaneously in the main memory. For each experiment the data are read only once from the mass storage device. When the transforms $G_k^T(s_j)$ and $L_k^T(s_j)$, and subsequently the values $M_{i,n}[G_k^T(s_j)]$ and $M_{i-1,n}[L_k^T(s_j)]$ are calculated, the actual data in real time are no longer needed. It takes little effort then to perform single-curve analysis of each experiment contemporaneously as all the required transforms are already determined.

The linear LAP2 can be implemented in two ways. The methods differ in the way the $n(q+1)$ unknowns $E_{k,i}$ and D_i are determined from the system given by eq. 15. In the first implementation, $E_{k,i}$ and D_i are calculated simultaneously. In most cases, the system will be overdetermined. A solution can then be obtained by applying least

squares. The lifetimes are obtained from D_i and the pre-exponentials thereafter from $E_{k,i}$. For a large number of experiments, memory restrictions may require reprogramming to provide efficient storage and handling of the sparse matrix of the system. An alternative can be provided as follows. For each experiment the elements $M_{i,n}[G_k^T(s_j)]$ and $M_{i-1,n}[L_k^T(s_j)]$ are saved, either in the main memory or on a mass storage device. The unknowns $E_{k,i}$ can be eliminated as suggested previously [14]. It can be shown that [14]

$$\sum_{i=0}^{n} \boldsymbol{M}_{k,i} D_i = 0 \tag{33}$$

with

$$\boldsymbol{M}_{k,i} = \left| M_{i,n}\left[G_k^T(s_j)\right] \;\; M_{i-1,n}\left[L_k^T(s_j)\right] \ldots \right.$$
$$\left. \ldots M_{0,n}\left[L_k^T(s_j)\right] \right|_{j=1,\ldots,n} \tag{34}$$

This will finally lead to an overdetermined system in the unknowns D_i. The symmetric matrix $(n \times n)$ of the normal equations in the least squares is built up while passing through the calculations for each experiment. Hence, the elements $\boldsymbol{M}_{k,i}$ do not have to be saved for each experiment. Estimates for D_i and hence for τ_j are readily obtained. These values and the stored coefficients $M_{i,n}[G_k^T(s_j)]$ and $M_{i-1,n}[L_k^T(s_j)]$ for each experiment are then used to set up a linear system from which $E_{k,i}$ can be determined for each experiment separately. An outline of this implementation of the linear LAP2 analysis is given in appendix E. Both implementations for the linear LAP2 give the same results.

It is also recommended that $M_{i,n}[G_k^T(s_j)]$ and $M_{i-1,n}[L_k^T(s_j)]$ are stored in the nonlinear LAP2, because the calculation of the transforms is the most time-consuming step in the analysis. In this way, a rapid evaluation of analyses with alternative linkages between the parameters can be performed. To obtain the solution of the overdetermined nonlinear system we use the Newton method where the derivatives in the linearization are calculated analytically. The increments for the parameters in each iteration are obtained by applying the Householder transformation [39] to the overdetermined system. Initial guesses for the nonlinear LAP2 may be estimated from the single curve analyses while the values for $M_{i,n}[G_k^T(s_j)]$ and $M_{i-1,n}[L_k^T(s_j)]$ are calculated.

All programs are implemented on an HP 1000 system (RTE-6VM) using HP Fortran 77. The programs for the described Laplace methods use double precision arithmetic (8 bytes). The values for the transform parameters were as follows: $s_1 = 0$ and increments Δ of 0.002 or 0.005. As in the original LAP2 [14], the Simpson integration rule was used in this work. The values for the transform parameters are restricted by the overflow and underflow condition on the computer.

3.3.2. Implementation of the NLLS global analysis

The procedure for global analysis using NLLS has been described in previous reports [20a,20b,26]. The NLLS implementation uses single precision. All NLLS analyses used Gaussian weighting.

4. Results

The performance of the global analysis by the LAP2-transform method was tested for multiexponential model functions on simulated and real data sets. In general, it was found that whenever the linear and nonlinear LAP2 were both applicable, the same estimates for the decay parameters were obtained. In the following, the results obtained by the described Laplace methods will be also compared with the NLLS estimates. The standard deviations σ_i of the latter are calculated under the linear approximation of the model. Wherever a deconvolution of real data against a measured excitation profile is performed, the wavelength dependence of the detection system is approximatively corrected for by the described Q-shift.

A first example concerns an experimental data set which was used by Knutson et al. [20a] to demonstrate the performance of the NLLS global analysis. The data consist of the fluorescence relaxations observed at six different emission wavelengths of a mixture of 9-cyanoanthracene and anthracene in methanol. In order to diminish the difference between the two lifetimes, potassium iodide was added as a quencher. Fig. 1 displays

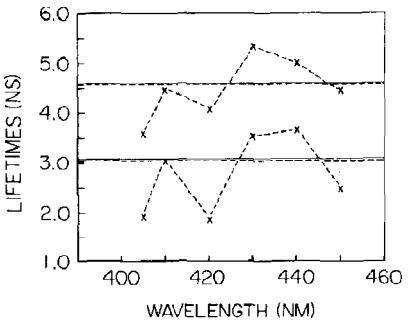

Fig. 1. Fluorescence lifetimes obtained from a mixture of 9-cyanoanthracene and anthracene in methanol quenched by KI: LAP2 single curve analysis (×), LAP2 global analysis (———) and NLLS global analysis (- - - - - -). The decays were measured over 511 channels; timing calibration, 0.102 ns/channel; full-width at half-maximum of the excitation profile, ≈ 2 ns; excitation wavelength, 337 nm.

the two fluorescence lifetimes recovered by analyzing each experiment separately by LAP2. A similar pattern was obtained by performing single-curve analysis using NLLS [20a]. However, the lifetimes observed with the individual unmixed compounds did not show any wavelength dependence and were found to be 4.6 ns for 9-cyanoanthracene and 3.2 ns for anthracene [20a]. Because of the relatively small difference between the two lifetimes, the results of the individual analyses are strongly influenced by the relative contributions of each fluorophore to the observed total intensities. The single-curve analysis by LAP2 and NLLS showed the same variation in the recovered lifetimes over the investigated wavelength region. The global type of analysis is the method of choice for this data set because the fluorescence lifetimes can be linked over all decay curves. The simultaneous analysis of the six curves by LAP2 yields lifetime values of 4.56 and 3.02 ns. Almost identical values were obtained by NLLS globals, 4.57 ns ($\sigma = 0.03$) and 3.07 ns ($\sigma = 0.02$).

To test the ability for resolving decay associated spectra, a mixture of anthracene ($\tau_1 = 3.7$ ns) and 9-cyanoanthracene ($\tau_2 = 11.5$ ns) in methanol was examined at room temperature. The solution was excited at 357 nm. Fluorescence decay curves were collected every 2 nm (with dwell times of only a few minutes) in the wavelength region 370–550 nm. The excitation profiles were measured contemporaneously (full-width at half-maximum ≈ 2 ns, peak value ≈ 800 counts). The fluorescence decay surface constructed from the 90 decay curves is represented in fig. 2. The 90 decay curves were analyzed simultaneously by LAP2 by linking the two fluorescence lifetimes over the complete decay

Table 1

Global analysis of simulated quadru-exponential decays

S.D. indicates the standard deviation estimated under the linear approximation. The channel width was 0.102 ns; the full-width of half-maximum of the used excitation profile was about 2 ns; the total number of counts in the 511 channels of the decays ranged from 1×10^6 to 2.8×10^6.

Simulation	Lifetimes (ns)				Amplitudes (ns^{-1})			
	1	3	7	10	Simulation no. 1			
					0.1	0.1	0.1	0.1
LAP2	0.8	3.0	7.0	9.9	0.10	0.11	0.09	0.11
NLLS	1.1	3.0	6.0	9.6	0.11	0.08	0.07	0.13
(S.D.)	(0.3)	(2.0)	(2.0)	(0.5)	(0.05)	(0.02)	(0.03)	(0.04)
LAP2	1.00	3.3	6.9	9.8	0.113	0.099	0.08	0.11
NLLS	1.02	3.0	7.0	10.0	0.103	0.095	0.10	0.10
(S.D.)	(0.05)	(0.2)	(0.2)	(0.2)	(0.008)	(0.006)	(0.01)	(0.01)
LAP2	0.95	2.9	7.1	10.2	0.102	0.098	0.12	0.09
NLLS	1.01	2.9	7.1	10.1	0.102	0.096	0.11	0.09
(S.D.)	(0.06)	(0.2)	(0.2)	(0.2)	(0.008)	(0.006)	(0.02)	(0.01)

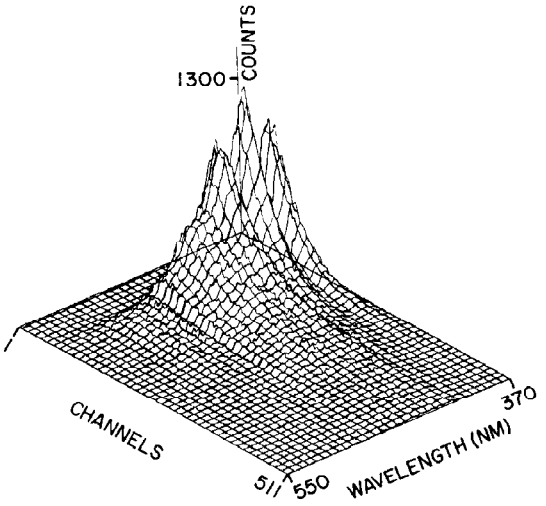

Fig. 2. Fluorescence decay surface of a mixture of 9-cyanoanthracene and anthracene as a function of emission wavelength and time (λ_{ex} = 357 nm, channel width = 0.102 ns). (For clarity, not all decay curves are shown.)

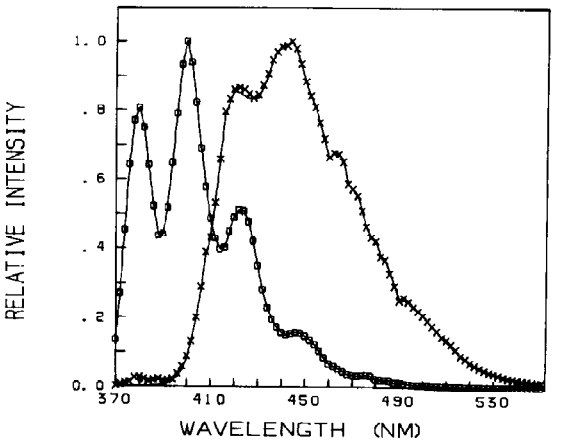

Fig. 3. Recovery of the technical fluorescence emission spectra 9-cyanoanthracene (×) and anthracene (○) by global analysis of the decay surface shown in fig. 3. The solid lines represent the spectra of the unmixed samples.

surface. According to eq. 32, the pre-exponentials then reflect the decay associated spectra. The total number of unknown parameters for this case is 182. The analysis with LAP2 took about 40 min on an HP 1000 multi-user system. The iterative NLLS global analysis required about 7 h. The recovered pre-exponentials are well superimposable on the spectra obtained from each component separately (fig. 3).

The ability of LAP2 to resolve four exponentials was also tested. Four simulations of quad-exponential decays were performed with common relaxation times of 1, 3, 7 and 10 ns and various sets of pre-exponential factors (see table 1). Single-curve LAP2 analyses for four exponentials yielded only three positive lifetimes with values in the neighborhood of 1, 3 and 9 ns. In the single-curve NLLS analyses a dependence of the final estimates on the initial guesses was noticed. This is usually taken as an indication that a simpler model deserves the preference [40]. Indeed, the three- and four-component model gave almost equal χ_r^2 val-

Amplitudes (ns^{-1})											
Simulation no. 2				Simulation no. 3				Simulation no. 4			
0.1	0.2	0.4	0.3	0.2	0.05	0.2	0.05	0.05	0.2	0.05	0.2
0.11	0.19	0.39	0.3								
0.14	0.15	0.32	0.4								
(0.06)	(0.07)	(0.08)	(0.1)								
0.13	0.19	0.35	0.33	0.206	0.05	0.190	0.058				
0.11	0.18	0.41	0.30	0.203	0.04	0.203	0.050				
(0.01)	(0.01)	(0.04)	(0.03)	(0.006)	(0.01)	(0.006)	(0.009)				
0.12	0.18	0.45	0.26	0.198	0.06	0.207	0.04	0.05	0.196	0.08	0.18
0.11	0.19	0.43	0.27	0.201	0.05	0.208	0.04	0.05	0.198	0.07	0.19
(0.01)	(0.01)	(0.05)	(0.04)	(0.008)	(0.01)	(0.008)	(0.01)	(0.01)	(0.006)	(0.03)	(0.02)

ues, where

$$\chi_r^2 = \frac{1}{\nu}\sum_i \frac{1}{\sigma_i^2}\left(y_i^0 - y_i^c\right)^2. \qquad (35)$$

σ_i are the standard deviations of the observed data y_i^0; the y_i^c are the corresponding calculated values and ν denotes the degrees of freedom in the analysis. In all cases the inappropriateness of the bi-exponential model was clearly indicated by significantly higher χ_r^2 values.

Much better performances of LAP2 and NLLS were obtained with global analyses. The results of the simultaneous analysis of two, three and four simulated decay curves are summarized in table 1. It can be seen that good recovery of the parameters is obtained by both methods, considering only two curves simultaneously. For all multiple anal-

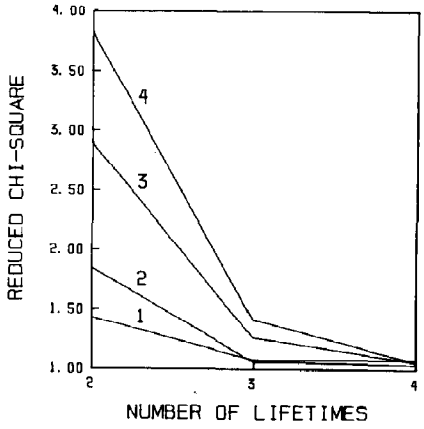

Fig. 4. The reduced χ_r^2 values resulting from the NLLS global analyses of the simulated decay curves in table 1. The numbers of curves considered in the global analysis are indicated as parameters near the curves.

Table 2

Reference deconvolution of a simulated tri-exponential decay

S.D. indicates the standard deviations obtained under the linear approximation of the model function. The deviations from the correct τ_R are indicated within brackets. The simulated decay ranged over 511 channels; the channel width was 0.102 ns; the full-width of half-maximum of the excitation profile was about 2 ns with a peak value of 20000 counts.

Simulation	α_1	α_2	α_3	τ_1 (ns)	τ_2 (ns)	τ_3 (ns)
	0.571	0.286	0.143	1	5	10
Lamp deconvolution						
LAP2	0.58	0.28	0.14	0.96	5.0	10.1
NLLS	0.58	0.29	0.13	1.01	5.2	10.1
(S.D.)	(0.01)	(0.01)	(0.01)	(0.02)	(0.2)	(0.2)
Reference deconvolution LAP2						
τ_R (ns)						
0.95 (−5%)	0.61	0.26	0.13	0.95	5.1	9.9
1	0.58	0.28	0.14	1.02	5.1	9.9
1.05 (+5%)	0.55	0.30	0.15	1.06	5.1	10.0
1.9 (−5%)	0.61	0.26	0.13	0.98	5.1	10.0
2	0.58	0.28	0.14	0.98	5.1	10.0
2.1 (+5%)	0.55	0.30	0.15	0.97	5.1	10.0
4.75 (−5%)	0.59	0.29	0.12	1.01	4.9	10.1
5	0.58	0.29	0.14	1.01	5.1	10.1
5.25 (+5%)	0.57	0.28	0.15	1.01	5.4	10.1
9.5 (−5%)	0.58	0.30	0.12	0.98	5.0	9.5
10	0.57	0.28	0.14	0.98	5.0	10.0
10.5 (+5%)	0.57	0.27	0.16	0.98	5.0	10.5

yses, the recovery of the simulation parameters is good and the results obtained by LAP2 and NLLS are quite comparable. Note the decrease in the uncertainty on the parameters when a third decay is included in the global analysis. The simultaneous analyses of three and four experiments yield almost the same standard deviations on the parameters. Also, the distinction between the models with three and four exponentials is more evident as the number of globalized curves is increased (fig. 4). The influence of initial guesses on the recovered parameters disappears in these NLLS global analyses.

The use of the deconvolution against the measured decay of a reference was first tested on simulated data. As pointed out in section 2, this type of deconvolution can be performed without knowing the lifetime of the reference, τ_R. In single-curve analysis the recovery of the simulation parameters was found to be poor when the unknown τ_R was close to one of the lifetimes of a multi-exponential decay. Therefore, we recommend the use of the reference deconvolution with unknown τ_R in single-curve analysis only for a mono-exponential decay. The same conclusion has been drawn for the reference deconvolution using NLLS [29]. The reference deconvolution with unknown τ_R may be better conditioned in a multiple-curve analysis due to the linkage between the parameters. In this approach one may consider either several decay experiments and a single non-characterized reference decay or several different reference decays in combination with the decay experiment(s). These procedures were not investigated as the emphasis in this contribution is on noniterative methods.

In the following, the reference deconvolution with known τ_R in multi-exponential analysis will be discussed. Its performance will be illustrated first on a simulation of a triple-exponential decay ($a_1 = 0.4$ ns^{-1}, $\tau_1 = 1$ ns, $a_2 = 0.2$ ns^{-1}, $\tau_2 = 5$ ns, $a_3 = 0.1$ ns^{-1}, $\tau_3 = 10$ ns). To investigate the effect of the value of the reference lifetime, four different mono-exponential reference decay curves were generated from the same excitation profile. One value for τ_R was chosen to be 2 ns and the three other values were taken equal to the lifetimes in the simulation of the triple-exponential decay. As τ_R in these reference deconvolutions is fixed, it is important to know how the values of the recovered parameters change with a deviation in τ_R from the correct value. For each of the four values for τ_R, two other values were considered: $1.05\tau_R$ and $0.95\tau_R$. The results of the regular lamp deconvolution by NLLS and LAP2 and of the 12 reference deconvolutions by LAP2 are summarized in table 2. The estimates obtained by the lamp deconvolution show that the simulation parameters can be recovered from the data. The four reference deconvolutions with the correct values for τ_R all perform equally well. This indicates that τ_R does not have to be shorter than the shortest lifetime appearing in the decay. The same conclusion was arrived at using the reference deconvolution by NLLS [29]. In addition, the reference deconvolution with known τ_R will recover the decay parameters quite well when τ_R is nearly equal or identical to a lifetime component in the decay. Acceptable parameter values are also obtained when the value for τ_R in the reference deconvolution deviates 5% from the correct value. In these cases, the differences between the estimates and the simulation parameters become more pronounced when the corresponding correct value of τ_R is smaller. It can be seen from table 2 that when the correct value of τ_R is equal to a lifetime in the decay, a reference deconvolution with an incorrect value for τ_R also returns practically the same incorrect value for the corresponding lifetime component with minimal effect on the other lifetimes.

To obtain values for unknown reference lifetimes, their corresponding decays can be decon-

Table 3

Deconvolution of two simulated mono-exponential decays against each other

Simulation parameters		Recovered values	
τ_1 (ns)	τ_2 (ns)	τ_1 (ns)	τ_2 (ns)
1	2	0.938	1.93
1	5	0.981	4.96
1	10	0.992	9.98
2	5	1.99	4.98
2	10	2.00	10.0
5	10	4.99	10.0

Table 4

Global analysis of fluorescence decay surface of 2-anilinonaphthalene in cyclohexane in the presence of 0.1 M ethanol at 25°C ($\lambda_{ex} = 337$ nm)

In the lamp deconvolutions with NLLS and LAP2, the same Q-shift was used. The reference deconvolutions were performed against the decay of 2-anilinonaphthalene in cyclohexane. A lifetime value of 4.35 ns was used. The decay curves contained 511 data points; the channel width was 0.05 ns; the full-width at half-maximum of the excitation profile was about 2 ns; the peak of the decays contained about 12000 counts. Standard deviations are obtained under the linear approximation of the model function and are denoted within parentheses.

λ_{em} (nm)	Q (ns)	NLLS lamp deconvolution			LAP2 lamp deconvolution			LAP2 reference deconvolution		
		$\tau_1 = 0.75$ ns (0.05) $\tau_2 = 1.95$ ns (0.02) $\tau_3 = 5.378$ ns (0.006)			$\tau_1 = 0.72$ ns $\tau_2 = 1.97$ ns $\tau_3 = 5.349$ ns			$\tau_1 = 0.70$ ns $\tau_2 = 1.96$ ns $\tau_3 = 5.322$ ns		
		α_1	α_2	α_3	α_1	α_2	α_3	α_1	α_2	α_3
360	0.000	0.33 (0.01)	0.54 (0.01)	0.122 (0.001)	0.35	0.52	0.121	0.33	0.55	0.121
370	0.005	0.14 (0.01)	0.65 (0.01)	0.205 (0.001)	0.21	0.59	0.200	0.14	0.65	0.208
380	0.039	−0.07 (0.01)	0.52 (0.01)	0.404 (0.003)	−0.05	0.52	0.430	−0.05	0.51	0.434
390	0.078	−0.08 (0.01)	0.23 (0.01)	0.687 (0.005)	−0.04	0.21	0.750	−0.04	0.20	0.754
400	0.099	−0.12 (0.01)	−0.03 (0.01)	0.854 (0.005)	−0.09	−0.05	0.855	−0.09	−0.07	0.847
420	0.095	−0.08 (0.01)	−0.25 (0.01)	0.670 (0.003)	−0.07	−0.26	0.669	−0.06	−0.27	0.668
430	0.120	0.02 (0.01)	−0.343 (0.009)	0.639 (0.003)	0.03	−0.345	0.621	0.02	−0.342	0.636

volved against each other by solving the system formed from eqs. 28 in an iterative way for τ_R. An example of this procedure is shown in table 3. Although both single lifetimes were freely adjustable in this iterative procedure, the recovery was very good when the lifetimes were sufficiently different. Reasonable values were still obtained for the case where the reference lifetimes were 1 and 2 ns.

An example of the reference deconvolution with known τ_R in global analysis will be demonstrated on fluorescence relaxation data of 2-anilinonaphthalene (2AN) in cyclohexane in the presence of small amounts of ethanol. It has been reported earlier that 2AN in this mixture undergoes a reversible two-state excited-state reaction [41]. This was based on single-curve analysis. We have now reinvestigated the behavior of 2AN in cyclohexane doped with 0.1 M ethanol at seven emission wavelengths at 25°C. The single-curve analyses by lamp deconvolution indicated that the data were well described by a double-exponential decay at all wavelengths. Simultaneous analysis of the curves at the various emission wavelengths by linking the two lifetimes yielded a rather high χ_r^2 value of 1.96. The surface of the residuals and their corresponding correlation functions revealed nonrandom distributions. Global analysis of the same data set for a tri-exponential decay model decreased the χ_r^2 value by the significant amount of 0.66 units and the structure in the residual surfaces disappeared. The parameter estimates obtained by lamp deconvolutions using NLLS and LAP2 are summarized in table 4. This table also shows the results obtained by a global analysis with the Laplace reference deconvolution. The reference solution was 2AN in cyclohexane with a lifetime value of 4.35 ns. Both types of deconvolution

yielded similar parameter values. It may be concluded that for the considered wavelength region the Q-shift correction was a valid approximation.

5. Conclusion

In this contribution, both an iterative and noniterative global analysis using modified Laplace transforms has been described. In many applications, only the fluorescence lifetimes need to be linked over the fluorescence decay surface. Attention is focussed on the noniterative Laplace global analysis although the iterative Laplace global analysis performs equally well. It has been shown that this unique noniterative global method compares very well with the NLLS global analysis. The linear implementation is very fast and is easy to use in practice because no initial guesses are required. Moreover, this method does not require extended memory facilities as does NLLS to perform efficiently. The number of experiments that can be globalized by the linear LAP2 is not restricted by the size of the logic memory of the processor. This makes the linear LAP2 global analysis the method of choice for obtaining decay associated spectra with a small dedicated computer. The convenience of the noniterative Laplace method is further enhanced by the capability of performing the deconvolution against the measured fluorescence decay of a reference. The same program can also be used to perform the regular lamp deconvolution by setting the lifetime of the reference formally equal to zero. To obtain statistics on the parameter estimates, the global analysis by LAP2 and NLLS can be combined. When the LAP2 global analysis provides the initial guesses for the iterative NLLS method, we find that the latter requires only a few iterations.

Appendix A: Derivation of eq. 4

For the model function $f(t)$ in eq. 2 the convolution product $g(t)$ can be written as

$$g(t) = \sum_{i=1}^{n} z_i(t) \tag{A1}$$

where

$$z_i(t) = \int_0^t I(u) a_i e^{-(t-u)/\tau_i} \, du \tag{A2}$$

is the contribution of the ith component in $f(t)$ to the convolution product $g(t)$. Note that $z_i(t)$ is purely mathematical and does not have to be associated with a particular excited species. Considering the restricted transformation over the interval $[0,T]$ of $g(t)$ yields

$$G^T(s) = \sum_{i=1}^{n} Z_i^T(s) \tag{A3}$$

Evaluating $Z_i^T(s)$ by partial integration and taking into account that

$$\frac{dz_i(t)}{dt} = -(1/\tau_i) z_i(t) + a_i I(t) \tag{A4}$$

gives

$$Z_i^T(s) = -(1/s) e^{-sT} z_i(T) - (1/s\tau_i) Z_i^T(s) + (a_i/s) L^T(s) \tag{A5}$$

Rearranging eq. A5 and performing the summation in eq. A3 gives eq. 4 when using $z_i(T) = a_i c_i$.

Appendix B: Derivation of eqs. 6 and 10

Eq. 4 can be rewritten as [14]

$$G^T(s_j) \sum_{i=1}^{n} s_j^i D_i(\tau) = L^T(s_j) \sum_{i=1}^{n} s_j^{i-1} E_i(a, \tau) - e^{-s_j T} \sum_{i=1}^{n} s_j^{i-1} H_i(a, \tau, c)$$
$$j = 1, \ldots, 3n \tag{B1}$$

with

$$H_i(\boldsymbol{a}, \tau, \boldsymbol{c}) = \sum_{1 \leqslant k_1 < k_2 < \ldots < k_i \leqslant n} \tau_{k_1}\tau_{k_2} \ldots \tau_{k_i}(a_{k_1}c_{k_1} + a_{k_2}c_{k_2} + \ldots + a_{k_i}c_{k_i}) \tag{B2}$$

It is shown in appendix C that eq. B1 can be derived in an alternative way which emphasizes the similarity between LAP2 and other transform methods. The functions $H_i(\boldsymbol{a}, \tau, \boldsymbol{c})$ can be eliminated from the linear system (eq. B1) by constructions of the following type for $1 \leqslant m \leqslant 2n$:

$$\begin{vmatrix} e^{-s_m T} & e^{-s_m T}s_m & \ldots e^{-s_m T}s_m^{n-1}G^T(s_m) + G^T(s_m)\left[\sum_{i=1}^{n} s_m^i D_i\right] - L^T(s_m)\left[\sum_{i=1}^{n} s_m^{i-1}E_i\right] \\ e^{-s_{m+1}T}e^{-s_{m+1}T}s_{m+1} & \ldots e^{-s_{m+1}T}s_{m+1}^{n-1}G^T(s_{m+1}) + G^T(s_{m+1})\left[\sum_{i=1}^{n} s_{m+1}^i D_i\right] - L^T(s_{m+1})\left[\sum_{i=1}^{n} s_{m+1}^{i-1}E_i\right] \\ \vdots & \vdots \\ e^{-s_{m+n}T}e^{-s_{m+n}T}s_{m+n} & \ldots e^{-s_{m+n}T}s_{m+n}^{n-1}G^T(s_{m+n}) + G^T(s_{m+n})\left[\sum_{i=1}^{n} s_{m+n}^i D_i\right] - L^T(s_{m+n})\left[\sum_{i=1}^{n} s_{m+n}^{i-1}E_i\right] \end{vmatrix} = 0 \tag{B3}$$

Expansion of eq. B3 along the last column yields

$$\sum_{j=0}^{n} (-1)^j \left\{ G^T(s_{m+j}) + G^T(s_{m+j})\left[\sum_{i=1}^{n} s_{m+j}^i D_i\right] - L^T(s_{m+j})\left[\sum_{i=1}^{n} s_{m+j}^{i-1}E_i\right]\left(\prod_{\substack{i=0 \\ i \neq j}}^{n} e^{-s_{m+i}T}\right) V_{j,n} \right\} = 0 \tag{B4}$$

where $V_{j,n}$ denotes the Vandermonde determinant,

$$V_{j,n} = \begin{vmatrix} 1 & s_m & \ldots & s_m^{n-1} \\ \vdots & \vdots & & \vdots \\ 1 & s_{m+j-1} & \ldots & s_{m+j-1}^{n-1} \\ 1 & s_{m+j+1} & \ldots & s_{m+j+1}^{n-1} \\ \vdots & \vdots & & \vdots \\ 1 & s_{m+n} & \ldots & s_{m+n}^{n-1} \end{vmatrix} \tag{B5}$$

It can be shown that [44]

$$V_{j,n} = \prod_{\substack{0 \leqslant l < k \leqslant n \\ l,k \neq j}} (s_{m+k} - s_{m+l}) \tag{B6}$$

Using transformation parameters satisfying

$$s_{m+k} - s_{m+l} = (k-1)\Delta \quad \Delta > 0 \tag{B7}$$

$V_{j,n}$ can be written as

$$V_{j,n} = \Delta^{n(n-1)/2} \frac{n!}{j!(n-j)!} \prod_{i=1}^{n} (n-i)! \tag{B8}$$

The final equations for E_i and D_i are obtained by substituting eq. B8 in eq. B4 and multiplying the result by the factor

$$\left[\prod_{i=1}^{n} e^{s_{m+i}}\right]\left[\Delta^{n(n-1)/2}\prod_{i=1}^{n}(n-i)!\right]^{-1} \tag{B9}$$

The final result will yield eq. 6 when using the notation defined by eq. 10.

Appendix C: Alternative derivation of eq. B1

It can be shown that for the model function $f(t)$ in eq. 2 the functions $g(t)$ and $l(t)$ are related by the following differential equation [15]

$$\sum_{i=0}^{n} D_i(\tau)g^i(t) = \sum_{i=1}^{n} E_i(\boldsymbol{a}, \tau)l^{(i-1)}(t) \tag{C1}$$

where $g^{(i)}(t)$ and $l^{(i)}(t)$ denote the ith time derivative of $g(t)$ and $l(t)$. In the different transform methods, eq. C1 is multiplied by a specific function $\rho(t)$ and an integration over time is performed [42,43], yielding

$$\sum_{i=0}^{n} D_i(\tau)\int_0^u \rho(t)g^{(i)}(t)\,\mathrm{d}t = \sum_{i=1}^{n} E_i(\boldsymbol{a}, \tau)\int_0^u \rho(t)l^{(i-1)}(t)\,\mathrm{d}t \tag{C2}$$

In LAP2, the integration is performed over the time interval $[0,T]$ and $\rho(t) = \exp(-st)$. This particular transform gives

$$\begin{aligned}\sum_{i=0}^{n} D_i(\tau)&\left\{s^i G^T(s) + \sum_{j=0}^{i-1} s^j\left[g^{(i-j-1)}(T)e^{-sT} - g^{(i-j-1)}(0)\right]\right\} \\ &= \sum_{i=1}^{n} E_i(\boldsymbol{a}, \tau)\left\{s^{i-1}L^T(s) + \sum_{j=0}^{i-2} s^k\left[l^{(i-j-2)}(T)\right.\right. \\ &\quad \left.\left.\times e^{-sT} - l^{(i-j-2)}(0)\right]\right\}\end{aligned} \tag{C3}$$

It can be shown that

$$g^{(i)}(t) = l(t)f^{(i)}(t) + \sum_{j=0}^{i-1} l^{(j)}(t)f^{(i-j-1)}(0), \tag{C4}$$

$$E_i(\boldsymbol{a}, \tau) = \sum_{j=0}^{n-i} D_{i+j}(\tau)f^{(j)}(0) \tag{C5}$$

The restricted transform $\boldsymbol{L}^T$ of the ith derivative of a function $p(t)$ is given by

$$\boldsymbol{L}^T(p^{(i)}) = s^i P^T(s) + \sum_{j=0}^{i-1} s^j\left[p^{(i-j-1)}(T)e^{-sT} - p^{(i-j-1)}(0)\right] \tag{C6}$$

Using eqs. C4–C6, an elaborate calculation which will not be given here, yields the following equations

$$\sum_{i=1}^{n} D_i(\tau) \sum_{j=0}^{i-1} s^j g^{(i-j-1)}(0) = \sum_{i=1}^{n-1} E_i(a, \tau) \sum_{j=0}^{i-2} s^j l^{(i-j-2)}(0), \tag{C7}$$

$$\sum_{i=1}^{n} D_i(\tau) \sum_{j=0}^{i-1} s^j g^{(i-j-1)}(T) = \sum_{i=1}^{n} s^{i-1} H_i(a, \tau, c), \tag{C8}$$

where $H_i(a, \tau, c)$ is defined by eq. B2. From eqs. C3, C7 and C8, eq. B1 is readily obtained.

Appendix D: Derivation of eq. 27

Considering the decay $g_R(t)$ of the reference solution, one may deduce from eq. 6 for $n = 1$ that

$$a_R \tau_R M_{0,1}\left[L^T(s_j)\right] = M_{0,1}\left[G_R^T(s_j)\right] + \tau_R M_{1,1}\left[G_R^T(s_j)\right] \tag{D1}$$

For $j = 0, \ldots, n-1$, eqs. D1 are multiplied by

$$\sum_{k=0}^{j} (-1)^k \frac{n!}{k!(n-k)!} s_k^{i-1} e^{j\Delta T} \tag{D2}$$

Adding respectively the left- and right-hand sides of the n resulting expressions leads to eq. 27 when using the property that

$$\sum_{j=0}^{n} (-1)^j \frac{n!}{j!(n-j)!} s_j^i = 0 \tag{D3}$$

for $0 \leqslant i \leqslant n-1$.
The property in eq. D3 can be proven from the identity

$$\left| s_j^i \; 1 \; s_j \; s_j^2 \; s_j^3 \ldots s_j^{n-1} \right|_{j=0,\ldots,n-1} = 0 \tag{D4}$$

for $0 \leqslant i \leqslant n-1$.
Expansion along the first column gives

$$\sum_{j=0}^{n} (-1)^j s_j^i V_{j,n} = 0 \tag{D5}$$

where $V_{j,n}$ is defined by eq. B5.

Use of the result in eq. B8 then leads to the justification of property in eq. D3.

Appendix E: Outline of the implementation of the linear LAP2

Step 1. For each decay experiment k:
- 1.1. Read $g_k(t)$ and $l_k(t)$ [or $g_{R,k}(t)$].
- 1.2. Calculate coefficients in eq. 28 ($\tau_R = 0$ if lamp deconvolution); save results on disk.
- 1.3. Calculate determinants $M_{k,i}$ defined in eq. 34.
- 1.4. Use $M_{k,i}$ to calculate contribution of experiment k to the matrix GLOBALD corresponding with the normal equations of the total system.

Step 2. Determine $D_i(\tau)$ from GLOBALD.

Step 3. Recover τ_j from $D_i(\tau)$ according to eq. 11.

Step 4. For each decay experiment k:
- 4.1. Read stored coefficients of eq. 28 from disk.
- 4.2. Use recovered values of τ_j to construct linear system for $E_{k,i}$.
- 4.3. Solve linear system for $a_{k,i}$.

Note added in proof (received 25 November 1985)

In a recent publication [45], we demonstrated that the species associated spectra (SAS) can also be obtained for systems undergoing excited-state reactions.

Acknowledgements

The authors wish to thank J.R. Knutson, R.P. DeToma and B.W. Turner for helpful discussions.

They would like to mention also L. Davenport, P. Neyroz, D. Walbridge and M. Han for providing the many test cases which are not mentioned in the text. N. Beechem is acknowledged for graphic art assistance. The work was supported by NIH grant no. GM11632 and NATO collaborative research grant RG. 85/0209. J.M.B. was supported by NIH training grant no. HD07103.

References

1 A.E. McKinnon, A.G. Szabo and D.R. Miller, J. Phys. Chem. 81 (1977) 1564.
2 D.V. O'Connor, W.R. Ware and J.C. André, J. Phys. Chem. 83 (1979) 1333.
3 M.G. Badea and L. Brand, Methods Enzymol. 61 (1979) 387.
4 M. Bouchy, Deconvolution-reconvolution (Conference Proceedings, Ecole Nationale Supérieure des Industries Chimique de l'Institut National Polytechnique de Lorraine, Nancy, France, 1982).
5 R.B. Cundall and R.E. Dale, Time-resolved fluorescence spectroscopy in biochemistry and biology (Plenum Press, New York, 1983).
6 J.N. Demas, Excited state lifetime measurements (Academic Press, New York, 1983).
7 A.E.W. Knight and B.K. Selinger, Spectrochim. Acta 27A (1971) 1223.
8 A. Grinvald and I.Z. Steinberg, Anal. Biochem. 59 (1974) 583.
9 I. Isenberg and R.D. Dyson, Biophys. J. 9 (1969) 1337.
10 W.P. Helman, Int. J. Radiat. Phys. Chem. 3 (1971) 283.
11 U.P. Wild, A.R. Holzwarth and H.P. Good, Rev. Sci. Instrum. 48 (1977) 1621.
12 J.C. André, L.M. Vincent, D.V. O'Connor and W.R. Ware, J. Phys. Chem. 83 (1979) 2285.
13 A. Gafni, R.L. Modlin and L. Brand, Biophys. J. 15 (1975) 263.
14 M. Ameloot and M. Hendrickx, Biophys. J. 44 (1983) 27.
15 B. Valeur and J. Moirez, J. Chim. Phys. Chim. Biol. 70 (1973) 500.
16 J.N. Demas and A.W. Adamson, J. Phys. Chem. 75 (1971) 2463.
17 P. Wahl and J.C. Auchet, Biochim. Biophys. Acta 285 (1972) 99.
18 F.J. Knorr and J.M. Harris, Anal. Chem. 53 (1981) 272.
19 J. Eisenfeld and C.C. Ford, Biophys. J. 26 (1979) 73.
20 a J.R. Knutson, J.M. Beechem and L. Brand, Chem. Phys. Lett. 102 (1983) 501; b J.M. Beechem, M. Ameloot and L. Brand, Anal. Instrum. 14 (1985) in the press.
21 J.P. Privat, P. Wahl, J.C. Auchet and R.H. Pain, Biophys. Chem. 11 (1980) 239.
22 C.W. Gilbert, in: Time-resolved fluorescence spectroscopy in biochemistry and biology, eds. R.B. Cundall and R.E. Dale (Plenum Press, New York, 1983) p. 605.
23 A.J. Cross and G.R. Fleming, Biophys. J. 46 (1984) 45.
24 M. Ameloot, H. Hendrickx, W. Herreman, H. Pottel, H. Van Cauwelaert and W. van der Meer, Biophys. J. 45 (1984) 525.
25 A. Arcioni and C. Zannoni, Chem. Phys. 88 (1984) 113.
26 J.M. Beechem, M. Ameloot and L. Brand, in: Excited state probes in biochemistry and biology, eds. A.G. Szabo and L. Masotti (Plenum Press, New York, 1986) in the press.
27 J.R. Knutson, D.G. Walbridge and L. Brand, Biochemistry 21 (1982) 4671.
28 P. Gauduchon and P. Wahl, Biophys. Chem. 8 (1975) 87.
29 R.W. Wijnaendts van Resandt, R.H. Vogel and S.W. Provencher, Rev. Sci. Instrum. 53 (1982) 1392.
30 L.J. Libertini and E.W. Small, Anal. Biochem. 75 (1984) 260.
31 M. Zuker, A.G. Szabo, L. Bramall, D.T. Krajcarski, and B.K. Selinger, Rev. Sci. Instrum. 56 (1985) 14.
32 G. Fodor, Laplace transforms in engineering, English translation by F. Petik (Akademiai Kiado, Budapest, 1965).
33 P. Wahl, J.C. Auchet and B. Donzel, Rev. Sci. Instrum. 45 (1974) 28.
34 A. Grinvald, Anal. Biochem. 75 (1976) 260.
35 D.R. James, D.R.M. Demmer, R.E. Verral and R.P. Steer, Rev. Sci. Instrum. 54 (1983) 1121.
36 P. Wahl, Biophys. Chem. 10 (1979) 91.
37 J.R. Lakowicz and H. Cherek, J. Biochem. Biophys. Methods 5 (1981) 19.
38 J.H. Easter, R.P. DeToma and L. Brand, Biophys. J. 16 (1976) 571.
39 W. Miller and C. Wrathall, Software for roundoff analysis of matrix algorithms (Academic Press, New York, 1980).
40 A.R. Gallant, Am. Stat. 29 (1975) 73.
41 R.P. DeToma and L. Brand, Chem. Phys. Lett. 47 (1977) 231.
42 J.L. Viovy, J.C. Andre, M. Bouchy, M. Roger and J. Bordet, in: Deconvolution-reconvolution, ed. M. Bouchy (Conference Proceeding, Ecole Nationale Supérieure des Industries Chimique de l'Institut Nationale Polytechnique de Lorraine, Nancy, France, 1982).
43 A.H. Kalantar, J. Luminescence 28 (1983) 411.
44 F.B. Hildebrand, Introduction to numerical analysis (McGraw-Hill, New York, 1974).
45 J.M. Beechem, M. Ameloot and L. Brand, Chem. Phys. Lett. 120 (1985) 466.